Topics in Catalysis (2022) 65:1899–1909
https://doi.org/10.1007/s11244-022-01704-4

ORIGINAL PAPER

Catalytic Reduction of Water Contaminants Using Green Gold Nanoparticles Mediated by Stem Extract of *Nepeta Leucophylla*

Deepika Kathuria[1] · Monika Bhattu[1] · Ajay Sharma[2] · Shweta Sareen[3] · Meenakshi Verma[1] · Sanjeev Kumar[4]

Accepted: 16 September 2022 / Published online: 2 October 2022

Abstract

Industrial waste effluents such as p-nitrophenol and heavy metals are considered as the main cause of water contamination. These contaminants lead to severe health hazardous effects to living organisms as well as to environment. For this purpose, the green synthesis of metallic nanoparticles has gotten more attention as a result of the rising need for non-toxic, rapid, simple, and environmentally compatible synthetic routes. In the present research, the basic objective is to detect the presence of these contaminants in water and to degrade the p-nitrophenol into a harmless by-product. The objectives were carried out using a a clean and sustainable method for making biogenic gold nanoparticles (AuNPs) from the stem extract of *N. leucophylla*. The electron microscopic and spectroscopic studies confirmed the formation of monodisperse and stable nanoparticles having size of 15–20 nm and a sharp absorption band at 548 nm. Further, the catalytic efficacy of the prepared nanoparticles was investigated towards the reduction of p-nitrophenol and for the reduction of heavy metal. The reduction of p-nitrophenol (100% conversion) in alkaline medium was observed using AuNPs as catalyst. The synthesized NPs showed a selective and sensitive colorimetric detection of Cr^{2+}. The limit of detection for Cr^{2+} was found to be 2.56 µM. This report suggests the potential of novel gold nanoparticles of *N. leucophylla* towards the water remediation.

Graphical abstract

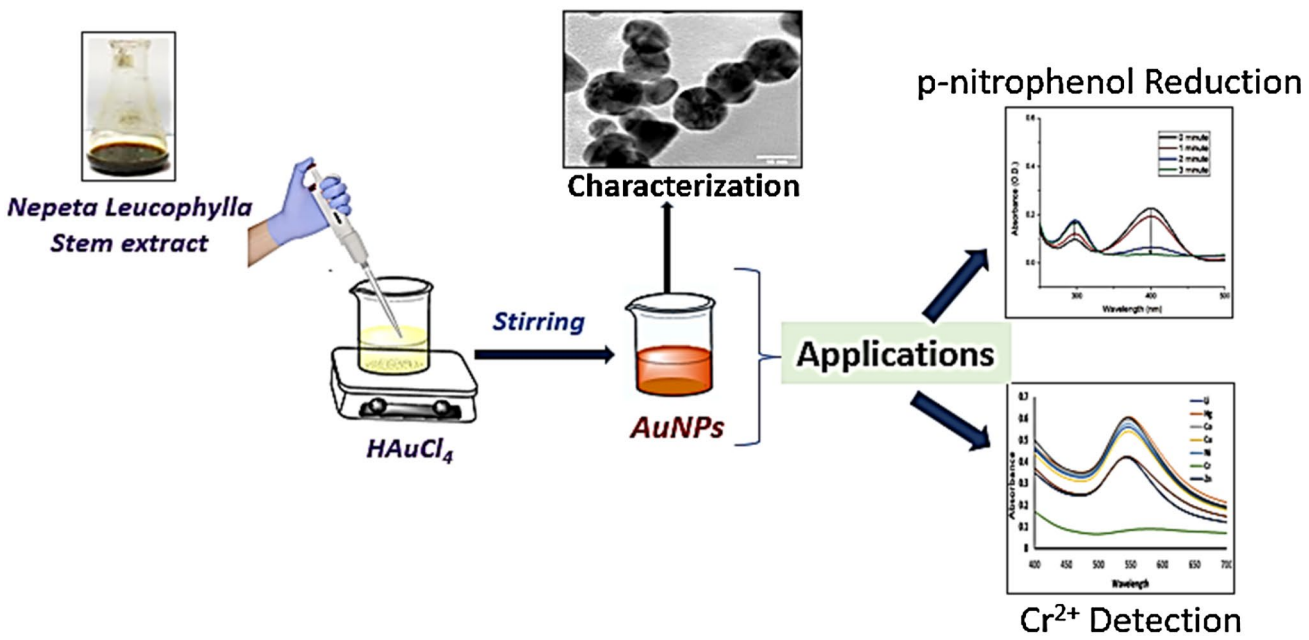

Keywords *N. leucophylla* extract · Green synthesis · Gold nanoparticles · p-Nitrophenol · Colorimetric detection

Extended author information available on the last page of the article

1 Introduction

The recent rapid expansion of industrialization and advances has resulted in the release of several contaminants in ecosystem, including water bodies. An extreme deterioration of the water quality has been resulted due to this rapid increase. Consequently, reducing water contaminants is of utmost concern and pollution control organisations give this issue a high importance [1]. The industries such as textile and coke furnace factories, dye industries, pulp and paper industries, tanneries, etc. contribute majorly towards the water contamination [2]. Due to urbanisation and broad industrialization the contamination caused by the synthetic inorganic and organic contaminants has become the imperative concern. Among the abovesaid contaminants, heavy metals ions and p-nitrophenol have been rated as the most harmful contaminants by United States Environmental Protection Agency (EPA 1980).

Long-term exposure to toxic discharge can result in delayed nervous system damage, neurological disorders, cancer, mutagenic changes, malformations in urban children The United States Environmental Protection Agency (EPA 1980) suggested the reduction of p-nitrophenol levels in natural water to less than 10 ng/L [3].

As a result of increased awareness, various researchers basically focus on the detection of heavy metals and removal of organic contaminants or their conversion of these organic contaminants into harmless by-products [4]. The efforts in the field of nanotechnology have been growing tremendously towards the detection and removal of these contaminants.

In the field of nanotechnology, metal nanoparticles (NPs) have been gaining tremendous importance in the field of scientific research and environmental applications. Among them, coinage metals (Au and Ag) NPs are much explored due to their distinct catalytic, electronic and optical characteristics [5].Nowadays gold nanoparticles (AuNPs) are employed as an effective redox catalyst [6–11], drug delivery [12–15], therapeutic applications [16–18] and also utilized in sensing of heavy metals and toxins. The synthesis of AuNPs generally consists of different physical and chemical methods. Among them the reduction of gold salts is the most common in which reducing agents such as citrate ion [19], sodium borohydride [20], ascorbic acid [21] and hydrazine [22]. These reducing agents reduces the Au(III) to Au(0) and also influences the shape and size of the AuNPs [23]. In spite of the successful outcomes of these aforementioned methods, these techniques suffer some disadvantages such as requirement of expensive chemicals, detrimental effect to the environment and human beings. Besides these, various biological processes are also reported in literature which includes the use of microorganisms for the synthesis of nanoparticles. However, these processes also involve a tedious procedure to procure the microbial cultures [24, 25].

All these negative impacts can be diminished by employing a green approach for the synthesis of nanoparticles. The green approach basically involves the synthesis of nanoparticles using the plant extract in which the plant extract offers several advantages such as easy accessibility, safe handling, non-toxicity. These plant extracts behave as reducing agent and capping agents which mediates the synthesis of these nanoparticles [26]. A number of medicinal plants such as geranium (*Pelargonium graveolens*) [27]; lemongrass (*Cymbopogon flexuosus*) [27]; Bengal gram beans (*Cicer arietinum*) [28]; *Pelargonium graveolens* [29] etc. have already been utilized for the synthesis of AuNPs.

Taking all these advantages of medicinal plants into consideration, we have chosen *Nepeta leucophylla* (a member of *Nepeta* class) for the synthesis of nanoparticles. Nepeta belong to the mint (*Lamiaceae*) family and consists of almost 300 species. *Nepeta leucophylla* is generally found in the Himalayan region of Uttarakhand, Himachal Pradesh, Jammu and Kashmir and Nepal. The major components present in the plant are dihydroiridodial diacetate (18.2%); iridodial dienol diacetate (7.8%); iridodial β-monoenol acetate (25.4%) [30]. The plant contains various bioactive components such as glycosides, terpenoids, flavonoids, steroids, and phenolic acids which also exhibit good catalytic activity and sensing properties. The therapeutic applications of these compounds exhibit the anti-inflammatory, antioxidant and anti-fungal potential. The application of the silver nanoparticles of *N. leucophylla* root extract were evaluated for its antioxidant potential. However, lack of research in the direction towards industrial waste remediation motivated us to use this ample Himalayan plant.

In this research, the methanolic extract of the *N. leucophylla* stem was taken which was employed to the preparation of AuNPs of stem extract of *N. leucophylla*. The synthesized AuNPs were further utilized in order to check their catalytic potential towards the reduction of p-nitrophenol and also to monitor their sensing behaviour towards the detection of heavy metals in aqueous medium (Scheme 1).

2 Experimental Section

2.1 Material and Methods

2.1.1 Chemicals and Reagents

The stem of *N. leucophylla* was collected from the Himalayan region at altitude of > 2000 m (Manimhesh hills of

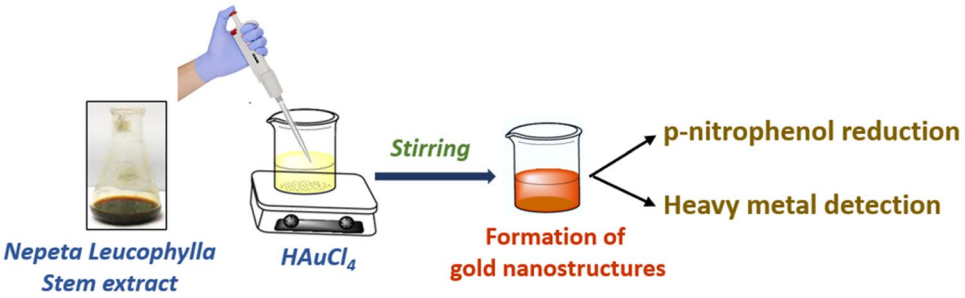

Scheme 1. Schematic diagram for the research methodology carried out in this work

Chamba; longitude 76_190-76.32_E and Hadsar, latitude 32_150-32.26_ N) of Himachal Pradesh, India. The voucher specimen (PUN58876) was identified by Dr. M. I. S. Saggoo, Department of Botany, Punjabi University, Patiala and deposited in the Herbarium of Punjabi University. The stems were shade dried at room temperature and processed into powder which was further preserved in an air tight container. 4-nitrophenol (4-NP), Silver nitrate ($AgNO_3$) and sodium borohydride ($NaBH_4$) were procured from Sigma Aldrich.

2.1.2 Preparation of Extract

The preserved stem of *N. leucophylla* was freshly extracted using ultrasound assisted extraction method (UAEM) and methanol as solvent which was further utilized for the preparation of AuNPs. The extraction was performed using Cole Parmer, USA (CPX 500 model, 500 W, 20 kHz) provided with standard Horn probe having replaceable tip and threaded end. The extraction was performed three times using different amount of solvent (150 mL, 75 mL and 75 mL) for different time intervals (30 min, 15 min and 15 min). The extracted liquid collected, filtered and the solvent was rota evaporated to obtained the concentrated extract.

2.1.3 Synthesis of Gold Nanoparticles

The AuNPs were synthesised by taking 50 mL of $HAuCl_4$ solution (1 mM) in four different beakers and was heated up to boiling under stirring conditions. When the solution was getting boiled, 1 mL, 2 mL, 3 mL and 4 mL of the stem extract (1 mg/mL) was added to the consecutive solutions of $HAuCl_4$. The solution was further kept under stirring conditions until the colour changes from yellow to pink Au(0).

2.2 Spectroscopic and Microscopic Characterisation of Gold Nanoparticles

The gold nanoparticles were characterised using UV–Visible Spectrophotometer (Shimadzu 2600). The size and the morphology of the nanoparticles was analysed using by transmission electron microscope (TEM).

2.3 Catalytic Potential for Reduction of p-Nitrophenol

The catalytic potential of synthesised AuNPs were evaluated against the reduction of p-nitrophenol. For this process, firstly the reaction conditions were optimized by varying the concentration of distilled water, p-nitrophenol, catalyst and reducing agent. Under the optimal conditions, the optimized amount of 4-nitrophenol, reducing agent, water and catalyst was added and the progress of reduction was monitored spectrophotometrically at different time intervals. On the completion of reduction of p-nitrophenol into p-aminophenol, the colour change has been observed from yellow to colourless.

2.4 Potential of Synthesised AuNPs for the Recognition of Heavy Metals

The synthesized nanoparticles were utilized to carry out the detection of heavy metals in water. For the recognition studies, firstly the 5 mM solution of the metal nitrates were prepared. The solution (100 µL, 5 mM) of metal nitrates was added to the synthesised green AuNPs in water (5 mL). U.V. Visible studies were performed in order to evaluate the recognition behaviour of these synthesized nanoparticles. No considerable change was observed in case of heavy metal except chromium. In case of the chromium (Cr^{2+}), a significant decrease was observed in the absorption spectra (absorbance becomes almost zero) which suggest the selective recognition potential of synthesized green AuNPs for the detection of chromium metal ion in aqueous media. Further, in order to check the specificity of the AuNPs, titration studies (1–50 µM), interference studies and effect of pH was also carried. The interference studies were performed by adding the potential competitive cations such as Li^{2+}, Cu^{2+}, Co^{2+}, Ni^{2+}, Zn^{2+}, Ba^{2+}, Pb^{2+} and Fe^{2+} to a mixture of AuNPs and Cr^{2+}.

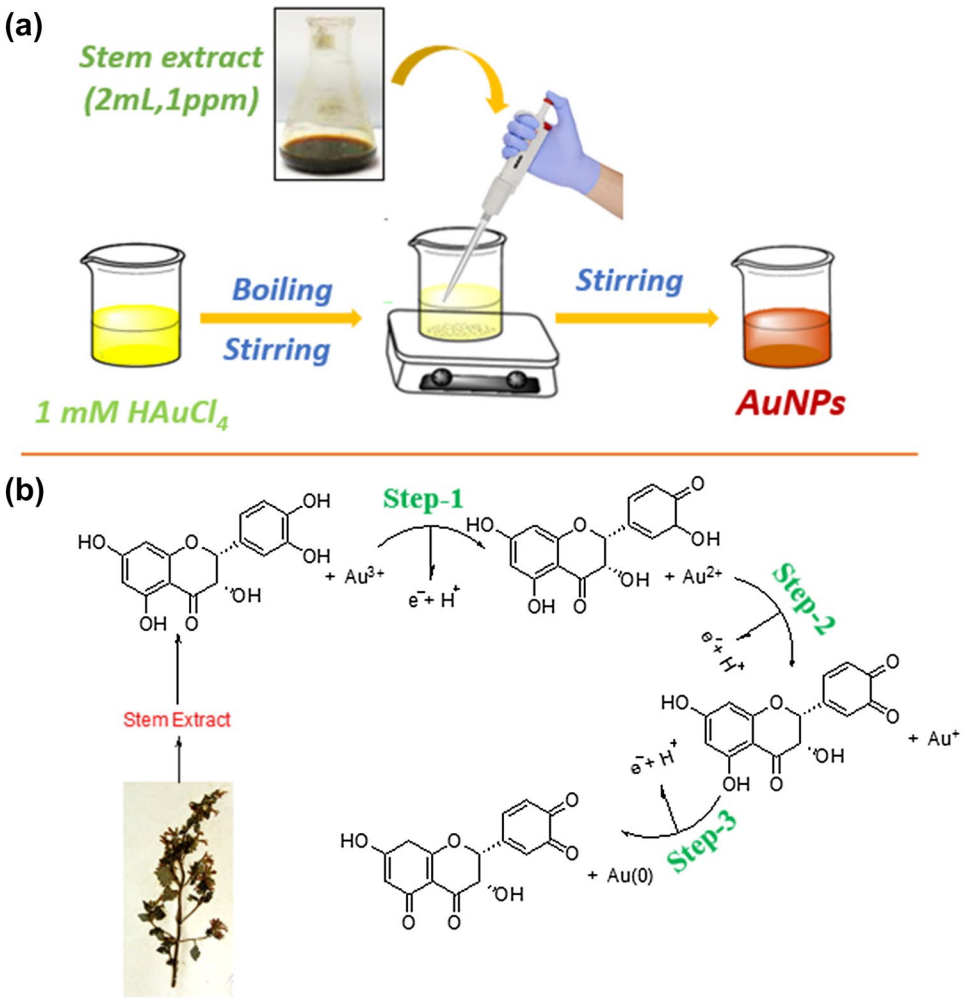

Scheme 2. **a** General preparation of gold nanoparticles mediated by *N. leucophylla* stem extract; **b** mechanism of formation

2.5 Antioxidant Potential

The antioxidant potential was evaluated using DPPH free radical scavenging assay which was determined with the help of UV–Visible Spectrophotometer 2600 (Shimadzu). For the determination of antioxidant potential three mixtures were prepared (2 samples and 1 blank). For evaluation of samples to the 3 mL of ethanolic solution of DPPH (0.004%) 200 µL of stem extract (1 mg/mL) or its AuNPs was added. For blank, 200 µL of ethanol was added in place of stem extract. All the prepared solutions ware incubated for 30 min in dark at room temperature. After incubation, the absorbance of the solutions was observed at 517 nm using UV–Visible spectrophotometer (Shimadzu). Using the observed absorbance, the inhibition percentage (I%) was calculated as following:

$$I\%\,[\text{DPPH free radical}] = \left[\left(A_C - A_S\right)/A_C\right] \times 100 \quad (1)$$

where, A_C and A_S are the absorbance of the control and samples/standard solutions respectively. The ascorbic acid and quercetin dehydrate were taken as standards. The % inhibition of each sample was estimated in triplicates.

3 Result and Discussion

3.1 Synthesis of AuNPs of *N. leucophylla* Stem Extract

The gold nanoparticles were synthesised by adding 2 mL of *N. leucophylla* stem extract to boiling solution of $HAuCl_4$ (1 mM, 50 mL) and the mixture was further heated for 10 min under stirring conditions until the colour changes from yellow to pink Au(0) was observed. The nanoparticles were centrifuged at 10,000 rpm for 15 min and

dried at 50 °C in hot air oven to obtain the solid AuNPs of *N. leucophylla* stem extract. The proposed mechanism for the formation of AuNPs is given in Scheme 2.

3.2 Optical Properties of AuNPs

The stem extract was utilized to reduce the Au(III) which is also responsible for the colour change from yellow to pink. The variation in colour from yellow to pink is due to the surface plasmon excitation (SPE) in gold atoms and is responsible for AuNPs formation [31]. The absorption maxima were observed at 548 nm (Visible region) (Fig. 1). The band gap energy for synthesized AuNPs was estimated to be 2.26 using Tauc's plot.

3.3 Structural Properties of AuNPs

Transmission Electron Microscopy (TEM) studies were employed to monitor the structural properties such as size and morphology of the synthesized AuNPs. Figure 2 shows that *N. leucophylla* stem extract synthesized a heterogeneous mixture of nanoparticles in size varying from 15 to 20 nm.

The TEM images revealed that the synthesised *N. leucophylla* stem extract AuNPs contain a mixture of spherical nanostructures, octagonal, hexagonal and truncated particles (Fig. 2). The formation of anisotropic nanostructures was owing to the occurrence of different biomolecules such as flavonoids and phenolic components which behave as a stabilizing and reducing agent which are responsible for the crystal growth and balancing of electrostatic forces during crystal growth [32]. Figure 3a display the electron diffraction (SAED) pattern of *N. leucophylla* stem extract AuNPs, where the presence of bright dots confirms the crystalline nature of the synthesized nanoparticles [33]. The EDX spectra of the synthesised AuNP's have been carried out in order to estimate the elemental composition. Analysis of EDX showed a strong signal at 2.1 keV which is attributed toward gold nanoparticles. The peaks between 0–0.5 keV indicated the presence of carbon, nitrogen, and oxygen (Fig. 3b) [34, 34, 35].

3.4 Catalytic Potential for the Reduction of p-Nitrophenol

The catalytic potential of the AuNPs was monitored by conducting the reduction of p-nitrophenol using $NaBH_4$ as reducing agent. The progress of the reaction was investigated using UV–Visible Spectrophotometer. In absence of catalyst, a sharp band was observed at 400 nm due to the formation of phenolate ion. On addition of catalyst, the band

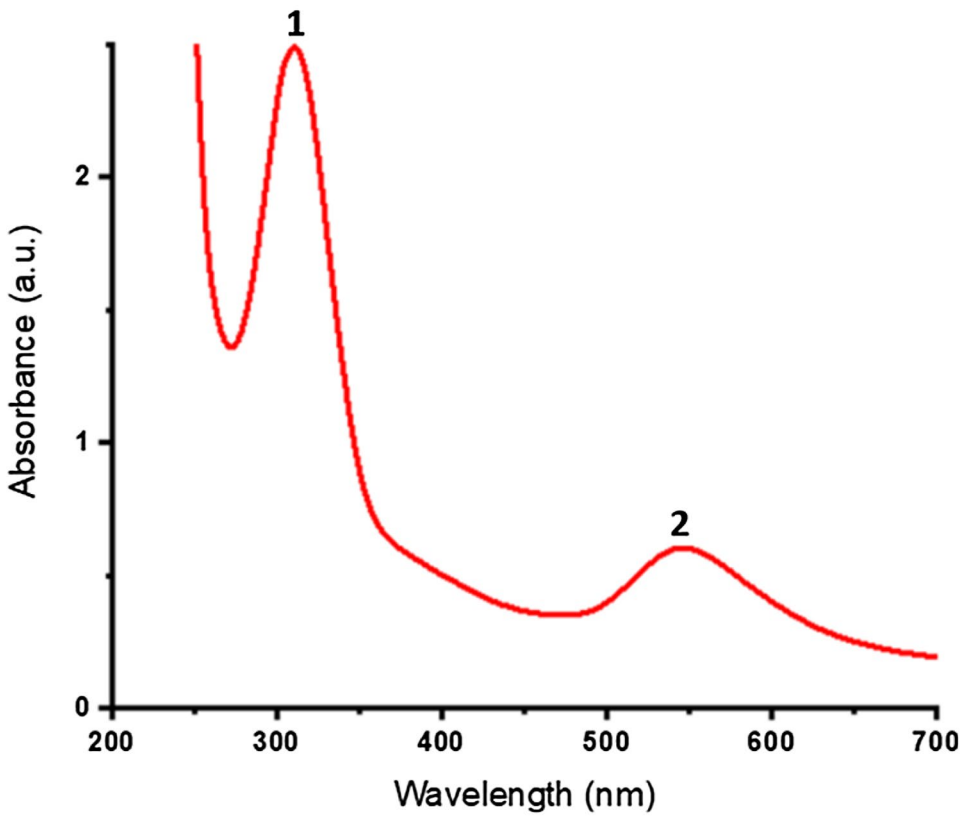

Fig. 1 UV–Visible spectra of the synthesized AuNPs exhibiting an absorption maximum at 548 nm (Peak 1 is for plant extract and peak 2 is for AuNPs)

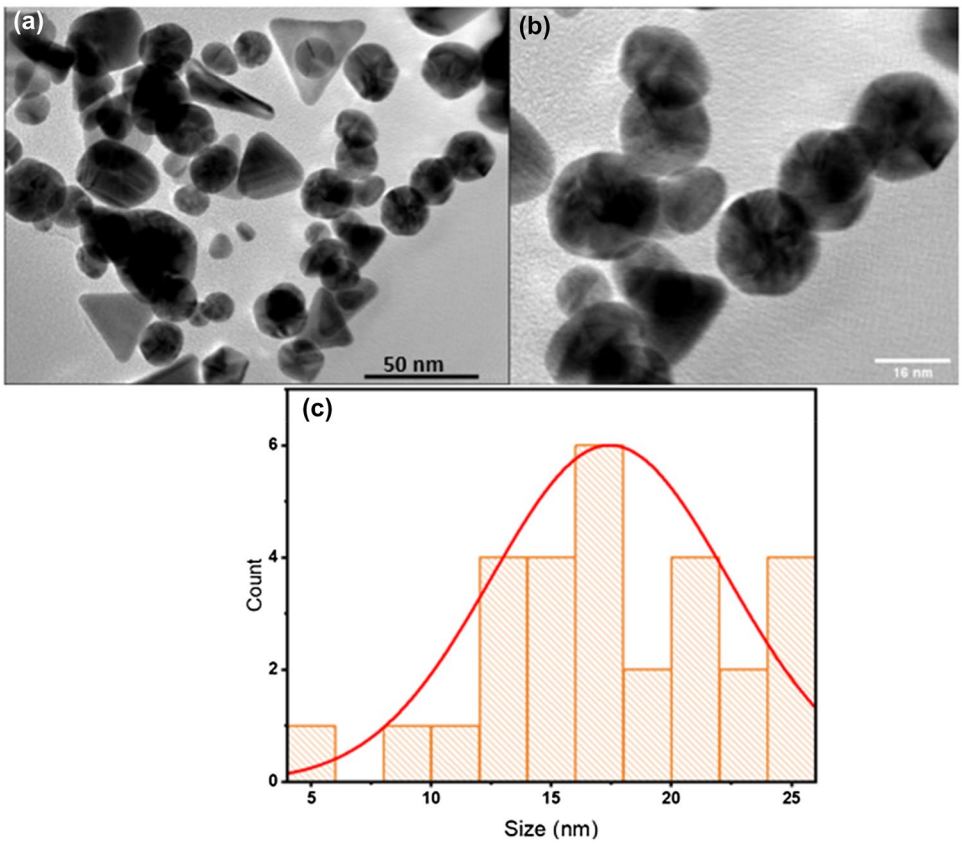

Fig. 2 TEM images of synthesized gold nanoparticles illustration the irregular shape and size of nanoparticles **a** at 50 nm; **b** at 16 nm; and **c** the size distribution curve showing the average size of nanoparticles varies from 15 to 20 nm

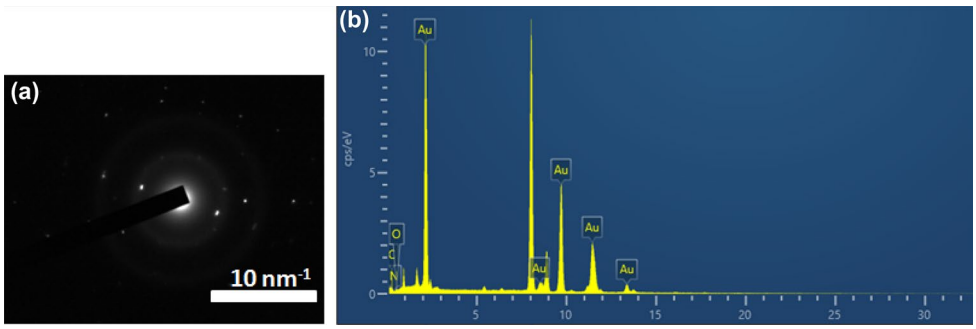

Fig. 3 **a** SAED pattern and **b** Energy dispersive spectra of *N. leucophylla* stem extract AuNPs

at 400 nm started decreasing and the appearance of a new band at 298 nm due to the aminophenol formation (Fig. 4). For monitoring the progress of reaction, firstly the reaction conditions were optimized by varying the amount of reducing agent, catalyst and reaction medium (water) (Table 1).

The best condition was found to be Entry no 3 (Table 1). Using the optimised conditions, the reduction was monitored at different time intervals. Within 3 min, the absorption band for phenolate ion completely disappeared which indicates the 100% conversion of p-nitrophenol into aminophenol.

AuNPs shows excellent catalytic properties towards the reduction of p-nitrophenol into p-aminophenol. The addition of reducing agent facilitates the deprotonation of p-nitrophenol into phenolate ion. The catalyst (AuNPs) present in the solution further reduces p-nitrophenol into p-aminophenol by adsorbing both the components on their surface. The presence of excess $NaBH_4$ is responsible for increase the pH of medium and hence inhibits the degradation of BH^{4-} ion (Scheme 3).

3.5 Kinetic Study of Catalysis

To compare the catalytic potential, a graph (Fig. 5a) was plotted by taking the normalized concentrations (ln C_o/ C)

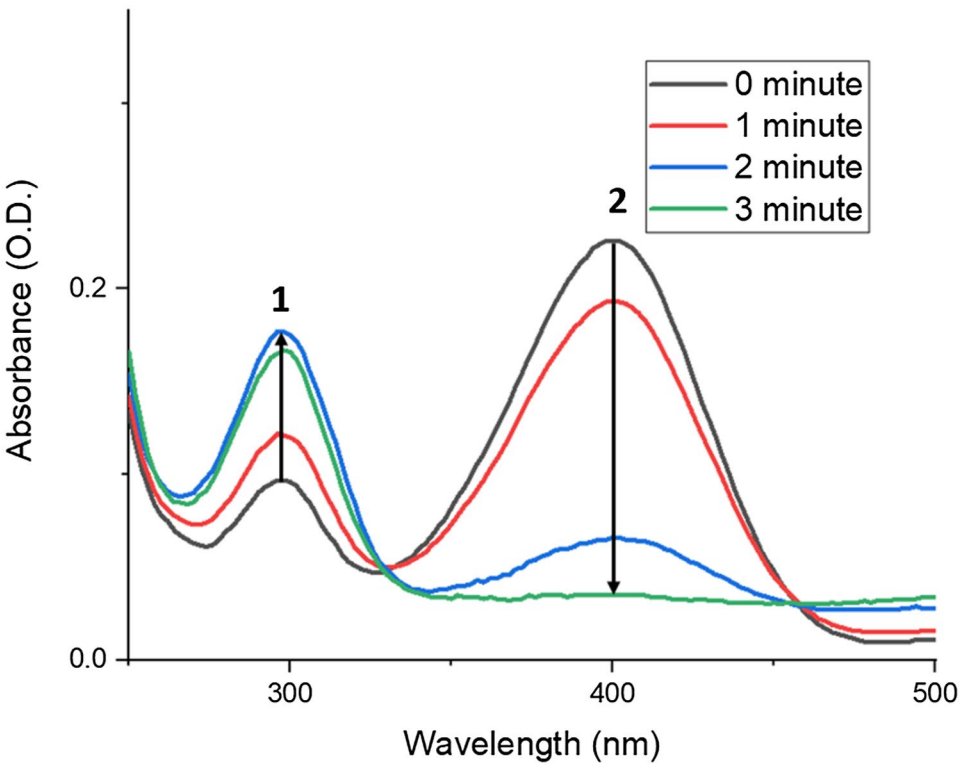

Fig. 4 UV–Visible spectra illustrating the reduction of p-nitrophenol mediated by synthesized AuNPs at varying time. Peak 1 belongs to p-aminophenol and peak 2 belongs to p-nitrophenol

Table 1 Conditions for optimization of catalytic reduction using AuNPs of *N. leucophylla*

Entry no.	2 mM p-nitrophenol (a* µL)	0.1 M $NaBH_4$ (a*, µL)	Catalyst (AuNPs, a* µL)	Time (min)
1	30	200	20	< 1
2	30	50	20	2
3	**30**	**20**	**20**	**3**
4	30	10	20	10
5	30	20	10	20

a* is the volume of the reagent used

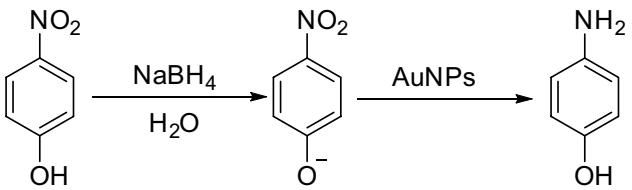

Scheme 3. Proposed mechanism for the p-nitrophenol reduction using nanoparticles as catalyst

(y-axis) and time (x-axis) where C_o and C indicates the initial and final concentrations of p-nitrophenol at time t. The plot indicates that the reaction follows the pseudo first order kinetics. Further the rate constant (k) was estimated using the linear graph equation of the plot ($\ln C/C_o = -kt$) which was found to be 0.326 min^{-1} (Fig. 5a). The time course study (Fig. 5b) depicts the rate of reduction of p-nitrophenol and the rate of formation of aminophenol which are inversely proportional to each other.

3.6 Photophysical Studies

The synthesized nanoparticles were utilized to demonstrate the colorimetric and spectrophotometric detection of heavy metal ions. For this purpose, 100 µL of the heavy metals ions solution (5 mM) such as Li^{2+}, Cu^{2+}, Co^{2+}, Ni^{2+}, Zn^{2+}, Ba^{2+}, Pb^{2+}, Cr^{2+} and Fe^{2+} were added the different vials of 5 mL of synthesized AuNPs solution. Primarily, the UV–Visible spectra of pure AuNPs solution and solution of AuNPs and heavy metal ions were recorded which showed an absorption maximum at 548 nm. There was no considerable change found in case of heavy metals except chromium (Cr^{2+}). The absorption peak intensity at 548 nm was completely diminished in case of Cr^{2+} (Fig. 6a).

Further, in order to confirm the sensitivity of the prepared AuNPs, titration studies, interference studies were performed. For the titration studies, subsequent addition of varying amount of Cr^{2+} (2 µL, 4 µL, 6 µL, 8 µL, 10 µL, 15 µL, 20 µL) was made to 1 mL of AuNPs solution. A normalised decrease was observed in the absorption intensity of the

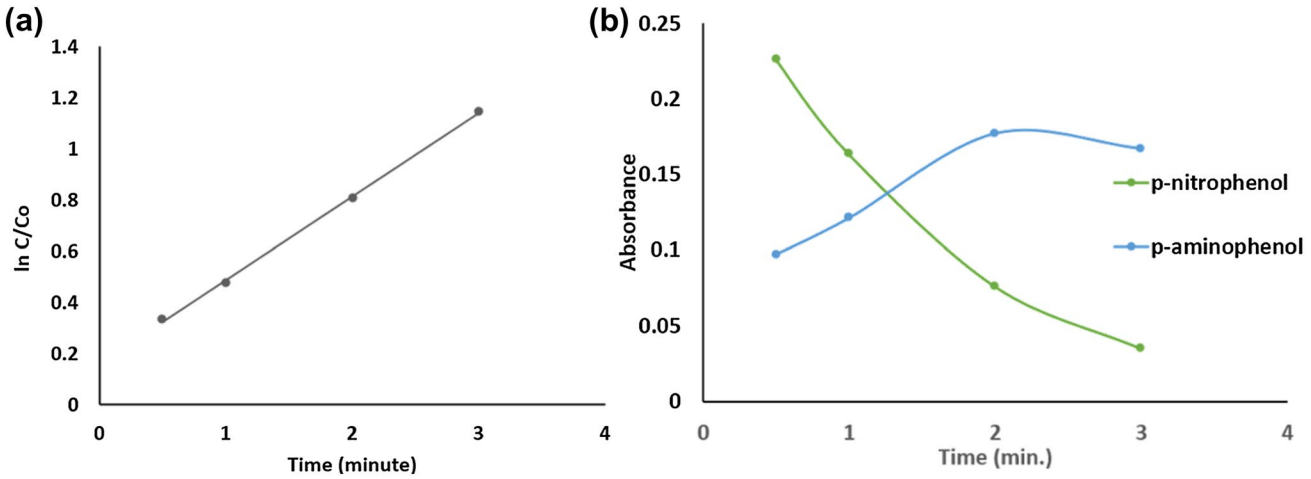

Fig. 5 **a** Plot of normalized concentration (ln Co/C) against reaction time (t) illustrating the linear relationship; **b** time course plot illustrating the concentration of p-nitrophenol left and p-aminophenol formed

AuNPs on increasing the concentration of Cr^{2+} solution in synthesized nanoparticles solution. (Fig. 6b).

Furthermore, to calculate the limit of detection (LOD) of the synthesized sensor, a linear calibration curve was plotted by taking the maximum absorption intensity (y-axis) of the AuNPs + Cr^{2+} solution at different concentrations of Cr^{2+} (x-axis) (Fig. 6c). The 3σ method was used to calculate the detection limit (LOD) (3.3 × Standard Deviation/Slope) and quantification limit (LOQ) (10 × Standard Deviation/Slope) were calculated using 3 sigma method and was observed to be 2.56 µM and 7.75 µM respectively.

To confirm the specificity and selectivity of the synthesized AuNPs towards the detection of Cr^{2+}, interference studies were carried out by adding the potential competing ions such as Li^{2+}, Cu^{2+}, Co^{2+}, Ni^{2+}, Zn^{2+}, Ba^{2+}, Pb^{2+} and Fe^{2+} to a solution of AuNPs + Cr^{2+}. However, negligible changes were observed in the absorption intensity of the AuNPs + Cr^{2+} (Fig. 6d).

The stability of the synthesized AuNPs towards the detection of Cr^{2+} was monitored against environmental factors such as pH and temperature. The synthesized NPs showed a stable response over a pH range of 1–9 (Fig. 7) and over a temperature varies from 15 to 50 °C.

Along with the spectrophotometric detection, a colorimetric colour changes were also monitored in presence of different metal ions such as Li^{2+}, Cu^{2+}, Co^{2+}, Ni^{2+}, Zn^{2+}, Ba^{2+}, Pb^{2+}, Cr^{2+} and Fe^{2+}. A considerable colour change (pink to colourless) was observed selectively in presence of Cr^{2+}. (Fig. 8).

Based on the UV spectra of the synthesized AuNPs, a possible mechanism is proposed for Cr^{2+} recognition. The presence of Cr^{2+} in AuNPs diminished the SPE band of AuNPs. The decrease may be attributed towards the metal–ligand interaction i.e., interaction of Cr^{2+} ions with the functional groups (–OH, –C=O) present on the surface of synthesized AuNPs. This interaction further leads to the aggregation of AuNPs which may be the possible reason for the disappearance of the colour. Various reports already found in literature for the colorimetric detection of chromium ion, however they involves a tedious synthesis process of nanoparticles via chemical based reaction [36–39].

3.7 Antioxidant Potential

The antioxidant potential was evaluated using the DPPH free radical scavenging assay which is based on the hydrogen atom releasing capacity of stem extract and NPs. The free radical of DPPH abstracts the hydrogen atom present in the antioxidants of plants which leads to the disappearance/reduction of colour intensity of DPPH solution. Lower the colour intensity, higher will be % antioxidant potential.

The calculated % antioxidant potential (Eq. 1) is found to be 54.47 ± 1.47% and 0.049% for stem extract and its AuNPs respectively. The stem extract possesses significant antioxidant potential, however, the antioxidant potential of its AuNPs is negligible which suggest that the antioxidants components in stem extract are utilized for the conversion of Au(3+) into Au(0) and thus was not available for the quenching of free radical of DPPH.

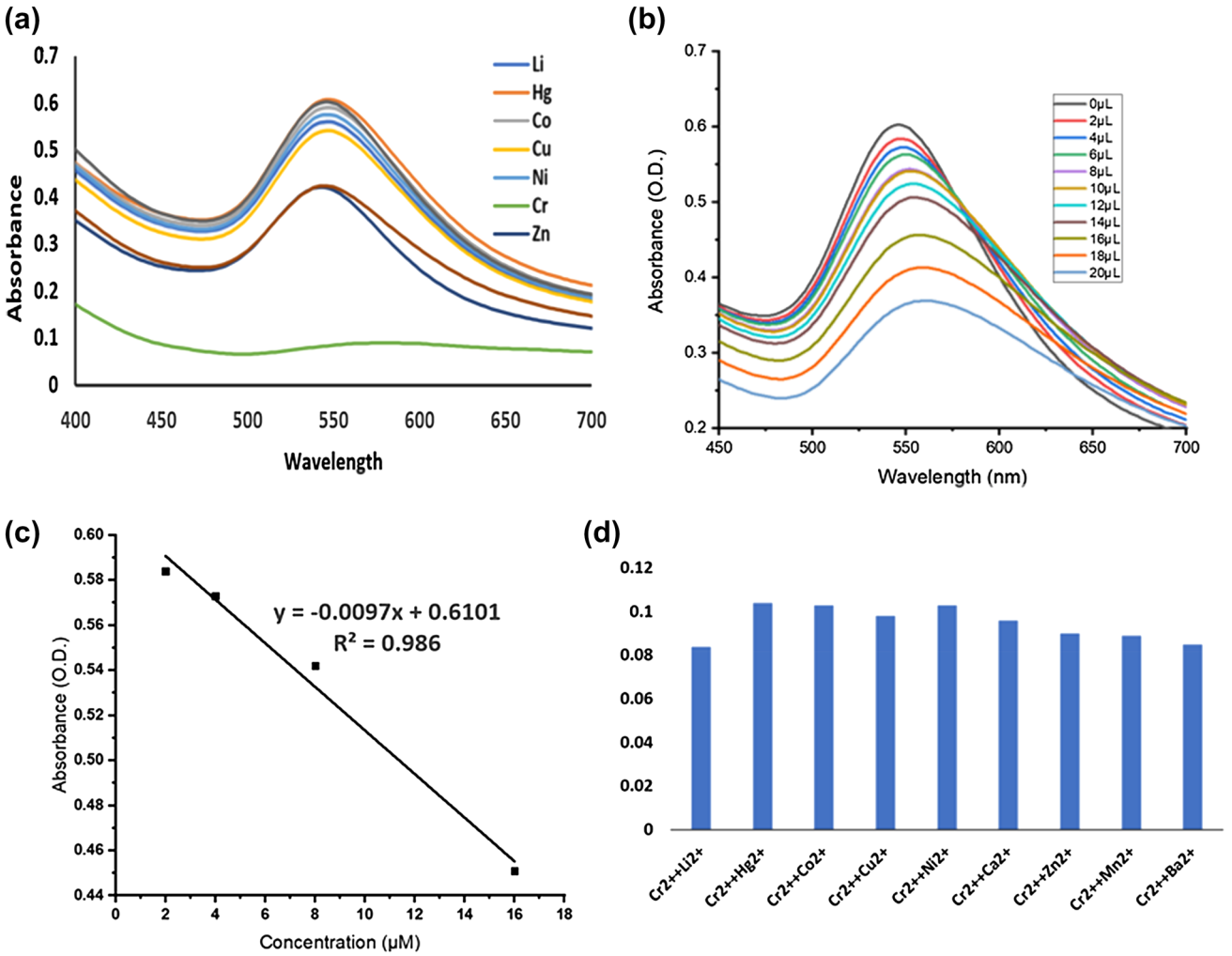

Fig. 6 **a** UV–Vis spectra of AuNPs on addition of various metal ions showing a specific decrease with Cr^{2+}; **b** spectra of AuNPs at various concentrations of Cr^{2+} ions (0–20 µM) illustrating a decrease in the absorbance intensity on increasing the concentration of metal ion; **c** calibration plot of absorbance versus concentration of Cr^{2+} ions; **d** bar graph of absorbance intensity of AuNPs + Cr^{2+} ions in presence of other potential ions showing negligible change

4 Conclusion

The current work reports the degradation of p-nitrophenol and reduction of Cr^{2+} using green nanoparticles. The hypothesis set for monitoring the degradation of p-nitrophenol was the appearance of p-aminophenol at a wavelength maximum of 298 nm. For carrying out the studies, *Nepeta leucophylla* stem extract mediated AuNPs were synthesized using one pot based green chemistry approach. Spectroscopic and TEM was utilized to evaluate the synthesis of AuNPs and surface morphology NPs respectively and showed an average size distribution of 15–20 nm. The synthesized NPs exhibit catalytic potential for the 100% conversion of 4-nitrophenol to 4-aminophenol using very low concentration (20 µL). The synthesised nanoparticles also possess selective recognition ability towards the detection of Cr^{2+} with a detection limit of 2.56 µM and also exhibit a significant colour variation from pink to colourless in presence of Cr^{2+} ions. The antioxidant potential was also evaluated, which showed that the gold nanoparticles do not exhibit any antioxidant activity in comparison to the methanolic extract of *N. leucophylla* stem.

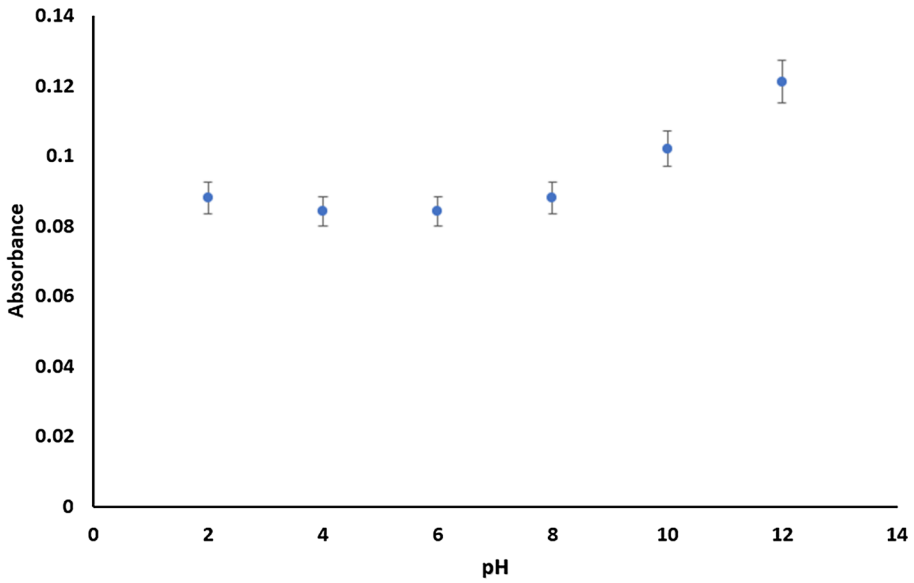

Fig. 7 UV–Vis. Spectra of AuNPs + Cr^{2+} ions in at a pH range varies from 0 to 12 showing the similar response over a range of 1–9

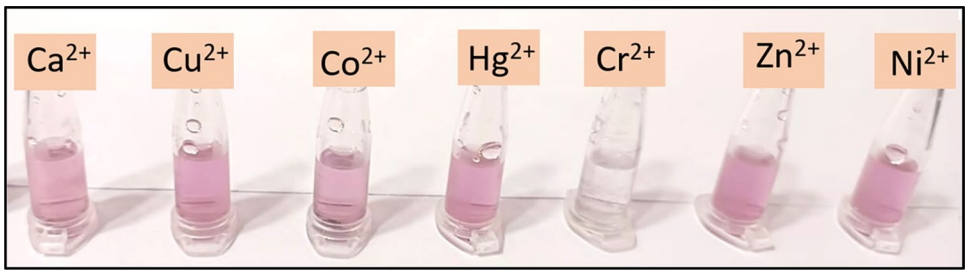

Fig. 8 Illustration of the colour change of AuNPs in different kind of metal ions showing the colour change from pink to colourless in presence of Cr^{2+}

References

1. Das A, Dey A (2020) P-Nitrophenol-bioremediation using potent Pseudomonas strain from the textile dye industry effluent. J Environ Chem Eng 8:103830. https://doi.org/10.1016/j.jece.2020.103830
2. Hanne LF, Kirk LL, Appel SM et al (1993) Degradation and induction specificity in actinomycetes that degrade p- nitrophenol. Appl Environ Microbiol 59:3505–3508. https://doi.org/10.1128/aem.59.10.3505-3508.1993
3. Sawal M (1986) General standards for discharge of environmental pollutants. Environ Rules 2:545–560
4. Liu Y, Luan J, Zhang C et al (2019) The adsorption behavior of multiple contaminants like heavy metal ions and p-nitrophenol on organic-modified montmorillonite. Environ Sci Pollut Res 26:10387–10397. https://doi.org/10.1007/s11356-019-04459-w
5. Singh J, Mehta A, Rawat M, Basu S (2018) Green synthesis of silver nanoparticles using sun dried tulsi leaves and its catalytic application for 4-Nitrophenol reduction. J Environ Chem Eng 6:1468–1474. https://doi.org/10.1016/j.jece.2018.01.054
6. Thompson DT (2007) Using gold nanoparticles for catalysis. Nano Today 2:40–43. https://doi.org/10.1016/S1748-0132(07)70116-0
7. Corma A, Garci H (2008) Supported gold nanoparticles as catalysts for organic reactions. Chem Soc Rev 37:2096–2126. https://doi.org/10.1039/b707314n
8. Stratakis M, Garcia H (2012) Catalysis by supported gold nanoparticles: beyond aerobic oxidative processes. Chem Rev 112:4469–4506. https://doi.org/10.1021/cr3000785
9. Szűcsab R, Balogh-Weisercd D, Sánta-Bellc E et al (2019) Green synthesis and in situ immobilization of gold nanoparticles and their application for the reduction of p-nitrophenol in continuous-flow mode. RSC Adv 9:9193
10. Suchomel P, Kvitek L, Prucek R et al (2018) Simple size-controlled synthesis of Au nanoparticles and their size-dependent catalytic activity. Sci Rep 8:1–11. https://doi.org/10.1038/s41598-018-22976-5
11. Lin C, Tao K, Hua D et al (2013) Size effect of gold nanoparticles in catalytic reduction of p-nitrophenol with NaBH4. Molecules 18:12609–12620. https://doi.org/10.3390/molecules181012609
12. Vasam M, Punagoti RA, Mourya R (2021) Biomedical applications of gold nanoparticles. Nanotechnol Life Sci 15:41–59. https://doi.org/10.1007/978-3-030-84262-8_2
13. Lopes-Nunes J, Agonia AS, Rosado T et al (2021) Aptamer-functionalized gold nanoparticles for drug delivery to gynecological carcinoma cells. Cancers (Basel) 13:1–16
14. Yafout M, Ousaid A, Khayati Y, El Otmani IS (2021) Gold nanoparticles as a drug delivery system for standard chemotherapeutics: a new lead for targeted pharmacological cancer treatments. Sci African 11:e00685. https://doi.org/10.1016/j.sciaf.2020.e00685
15. Mulikova T, Abduraimova A, Molkenova A et al (2021) Mesoporous silica decorated with gold nanoparticles as a promising nanoprobe for effective CT X-ray attenuation and potential drug delivery. Nano-Struct Nano-Obj 26:100712
16. Muddapur UM, Alshehri S, Ghoneim MM et al (2022) Plant-based synthesis of gold nanoparticles and theranosticapplications: a review. Molecules 27:1391

17. Liu XY, Wang JQ, Ashby CR et al (2021) Gold nanoparticles: synthesis, physiochemical properties and therapeutic applications in cancer. Drug Discov Today 26:1284–1292. https://doi.org/10.1016/j.drudis.2021.01.030
18. Ielo L, Rando G, Giacobello F et al (2021) Synthesis, chemical-physical characterization, and biomedical applications of functional gold nanoparticles: a review. Molecules 26:5823
19. Tyagi H, Kushwaha A, Kumar A, Aslam M (2016) A facile pH controlled citrate-based reduction method for gold nanoparticle synthesis at room temperature. Nanoscale Res Lett 11:1–11. https://doi.org/10.1186/s11671-016-1576-5
20. Aryal S, Remant BKC, Dharmaraj N et al (2006) Spectroscopic identification of SAu interaction in cysteine capped gold nanoparticles. Spectrochim Acta - Part A Mol Biomol Spectrosc 63:160–163. https://doi.org/10.1016/j.saa.2005.04.048
21. Malassis L, Dreyfus R, Murphy RJ et al (2016) One-step green synthesis of gold and silver nanoparticles with ascorbic acid and their versatile surface post-functionalization. RSC Adv 6:33092–33100. https://doi.org/10.1039/c6ra00194g
22. Sohn JS, Kwon YW, Il JJ, Jo BW (2011) DNA-templated preparation of gold nanoparticles. Molecules 16:8143–8151. https://doi.org/10.3390/molecules16108143
23. Kim H et al (2016) Concentration effect of reducing agents on green synthesis of gold nanoparticles: size, morphology, and growth mechanism. Nanoscale Res Lett 11:33092–33100. https://doi.org/10.1186/s11671-016-1393-x
24. Spring S, Schleifer KH (1995) Diversity of magnetotactic bacteria. Syst Appl Microbiol 18:147–153. https://doi.org/10.1016/S0723-2020(11)80386-3
25. Krishnaraj C, Jagan EG, Rajasekar S et al (2010) Synthesis of silver nanoparticles using *Acalypha indica* leaf extracts and its antibacterial activity against water borne pathogens. Colloids Surf B 76:50–56. https://doi.org/10.1016/j.colsurfb.2009.10.008
26. Singh J, Dhaliwal AS (2019) Novel green synthesis and characterization of the antioxidant activity of silver nanoparticles prepared from *Nepeta leucophylla* root extract. Anal Lett 52:213–230. https://doi.org/10.1080/00032719.2018.1454936
27. Shankar SS, Rai A, Ankamwar B et al (2004) Biological synthesis of triangular gold nanoprisms. Nat Mater 3:482–488. https://doi.org/10.1038/nmat1152
28. Ghule K, Ghule AV, Liu JY, Ling YC (2006) Microscale size triangular gold prisms synthesized using bengal gram beans (*Cicer arietinum* L.) extract and $HAuCl_4{\cdot}3H_2O$: a green biogenic approach. J Nanosci Nanotechnol 6:3746–3751. https://doi.org/10.1166/jnn.2006.608
29. Gardea-Torresdey JL, Tiemann KJ, Gamez G et al (1999) Gold nanoparticles obtained by bio- precipitation from gold (III) solutions. J Nanoparticle Res 1:397–404
30. Sharma A, Cannoo DS (2017) A comparative study of effects of extraction solvents/techniques on percentage yield, polyhenolic composition, and antioxidant potential of various extracts obtained from stems of Nepeta leucophylla: RP-HPLC-DAD assessment of its polyhenolic constituents. J Food Biochem 41:1–12. https://doi.org/10.1111/jfbc.12337
31. Jana J, Ganguly M, Pal T (2016) Enlightening surface plasmon resonance effect of metal nanoparticles for practical spectroscopic application. RSC Adv 6:86174–86211. https://doi.org/10.1039/c6ra14173k
32. Lee SY, Krishnamurthy S, Cho CW, Yun YS (2016) Biosynthesis of gold nanoparticles using *Ocimum sanctum* extracts by solvents with different polarity. ACS Sustain Chem Eng 4:2651–2659. https://doi.org/10.1021/acssuschemeng.6b00161
33. Hashem AH, Shehabeldine AM, Ali OM, Salem SS (2022) Synthesis of chitosan-based gold nanoparticles: antimicrobial and wound-healing activities. Polymers (Basel) 14:2293. https://doi.org/10.1016/B978-0-444-63285-2.00002-X
34. Suriyakala G, Sathiyaraj S, Babujanarthanam R et al (2022) Green synthesis of gold nanoparticles using *Jatropha integerrima* Jacq. flower extract and their antibacterial activity. J King Saud Univ Sci 34:101830. https://doi.org/10.1016/j.jksus.2022.101830
35. Vimalraj S, Ashokkumar T, Saravanan S (2018) Biogenic gold nanoparticles synthesis mediated by Mangifera indica seed aqueous extracts exhibits antibacterial, anticancer and anti-angiogenic properties. Biomed Pharmacother 105:440–448. https://doi.org/10.1016/j.biopha.2018.05.151
36. Dong C, Wu G, Wang Z et al (2016) Selective colorimetric detection of Cr(III) and Cr(VI) using gallic acid capped gold nanoparticles. Dalt Trans 45:8347–8354. https://doi.org/10.1039/c5dt04099j
37. Ravindran A, Elavarasi M, Prathna TC et al (2012) Selective colorimetric detection of nanomolar Cr (VI) in aqueous solutions using unmodified silver nanoparticles. Sens Actuators B Chem 166–167:365–371. https://doi.org/10.1016/j.snb.2012.02.073
38. Shrivas K, Sahu S, Patra GK et al (2016) Localized surface plasmon resonance of silver nanoparticles for sensitive colorimetric detection of chromium in surface water, industrial waste water and vegetable samples. Anal Methods 8:2088–2096. https://doi.org/10.1039/c5ay03120f
39. Wang X, Wei Y, Wang S, Chen L (2015) Red-to-blue colorimetric detection of chromium via Cr (III)-citrate chelating based on Tween 20-stabilized gold nanoparticles. Colloids Surf A 472:57–62. https://doi.org/10.1016/j.colsurfa.2015.02.033

Authors and Affiliations

Deepika Kathuria[1] · Monika Bhattu[1] · Ajay Sharma[2] · Shweta Sareen[3] · Meenakshi Verma[1] · Sanjeev Kumar[4]

✉ Deepika Kathuria
niperdeepika12@gmail.com

[1] University Centre for Research and Development, Chandigarh University, Gharuan, Punjab 140413, India

[2] Department of Chemistry, Sant Longowal Institute of Engineering and Technology, Longowal, Punjab 148106, India

[3] School of Chemistry and Biochemistry, Thapar University, Patiala, Punjab 147004, India

[4] Swift School of Pharmacy, Rajpura, Punjab 140401, India